J. Electroanal. Chem., 295 (1990) 409–414
Elsevier Sequoia S.A., Lausanne

Preliminary note

Theoretical neutron flux levels, dose rates, and metal foil activation in electrochemical cold fusion experiments

M.H. Miles *

Chemistry Division, Research Department, Naval Weapons Center, China Lake, CA 93555 (U.S.A.)

R.E. Miles

Nuclear Safety Department, E.G. and G. Rocky Flats Inc., Rocky Flats Plant, Golden, CO 80402 (U.S.A.)

(Received 12 June 1990; in revised form 25 September 1990)

INTRODUCTION

The electrochemically induced cold nuclear fusion process reported by Fleischmann, Pons, and Hawkins [1] is being investigated in many laboratories. The possible exposure to neutrons and other harmful radiation in cold fusion experiments is a matter of significant concern. A method that can provide conclusive evidence for the production of neutrons in these experiments is also needed. Therefore, theoretical calculations of neutron flux rates and the corresponding neutron dose rates were performed for various surfaces of our electrochemical calorimetric cell. This cell consisted of a palladium rod cathode ($d = 0.635$ cm, $l = 1.1$ cm) surrounded by a platinum coil anode in a glass tube that initially contained 18–20 g of 0.1 M LiOD + D_2O. A secondary compartment or gap surrounded the electrochemical cell and contained 68–70 g of distilled water. The two glass compartments were contained within a polyethylene bottle ($d = 7.5$ cm, $h = 16$ cm) filled with insulating material (vermiculite and styrofoam). A rubber stopper was used to close off the top of the cell. This cold fusion bottle was surrounded by water in a constant temperature bath during experiments. An excess rate of heating that averaged 0.39 W/cm^3 over a 9-day period for the Pd/D_2O + LiOD system was observed using this cell design [2].

NEUTRON FLUX AND DOSE CALCULATIONS

Fusion of deuterium nuclei to produce neutrons normally occurs by the reaction [1,3]

$$^2D + {}^2D \rightarrow {}^3He\ (0.817\ MeV) + n\ (2.452\ MeV) \quad (1)$$

* To whom correspondence should be addressed.

0022-0728/90/$03.50

TABLE 1

Neutron flux levels for the surface of the Pd rod, D_2O cell, side and top of the polyethylene bottle assuming a source of 10^4 neutrons per second

Group (neutron energies)	Neutron flux/n cm^{-2} s^{-1}			
	Pd surface	D_2O cell	Side of bottle	Top of bottle
1 (> 3 MeV)	9.325×10^{2}	1.996×10^{2}	3.965	2.177×10^{-1}
2 (1.4–3 MeV)	1.451×10^{3}	5.408×10^{2}	6.337	3.234×10^{-1}
3 (0.9–1.4 MeV)	7.059×10^{2}	1.563×10^{2}	2.904	9.444×10^{-2}
4 (0.4–0.9 MeV)	8.095×10^{2}	1.905×10^{2}	3.674	1.076×10^{-1}
5 (0.1–0.4 MeV)	4.759×10^{2}	1.271×10^{2}	2.945	9.235×10^{-2}
6 (17–100 KeV)	9.445×10^{1}	3.237×10^{1}	1.319	5.028×10^{-2}
7 (3–17 KeV)	7.610	7.644	6.228×10^{-1}	2.170×10^{-2}
8 (0.55–3 KeV)	3.337	3.950	3.563×10^{-1}	1.817×10^{-2}
9 (0.1–0.55 KeV)	1.441	2.152	2.092×10^{-1}	1.108×10^{-2}
10 (30–100 eV)	5.499×10^{-1}	9.374×10^{-1}	9.950×10^{-2}	1.017×10^{-2}
11 (10–30 eV)	5.554×10^{-1}	5.685×10^{-1}	6.250×10^{-2}	3.463×10^{-3}
12 (3–10 eV)	3.756×10^{-1}	4.060×10^{-1}	4.712×10^{-2}	4.107×10^{-3}
13 (1–3 eV)	2.669×10^{-1}	2.595×10^{-1}	3.209×10^{-2}	2.610×10^{-3}
14 (0.4–1 eV)	1.113×10^{-1}	1.156×10^{-1}	2.090×10^{-2}	3.624×10^{-3}
15 (0.1–0.4 eV)	1.891×10^{-1}	2.727×10^{-1}	2.880×10^{-2}	1.743×10^{-3}
16 (< 0.1 eV)	3.056×10^{-1}	4.068×10^{-1}	3.443×10^{-2}	4.632×10^{-3}
Totals	4.484×10^{3}	1.263×10^{3}	2.266×10^{1}	9.671×10^{-1}

However, since the exact nature of the cold fusion reaction within the palladium lattice is unknown, we assumed a neutron energy spectrum given by

$$\chi(E) = 0.770E^{1/2}\, e^{-0.776E} \tag{2}$$

that yields an average neutron energy of 2.0 MeV.

The neutron flux levels at four different surfaces of the electrochemical calorimetric cell are presented in Table 1 and illustrated in Fig. 1. These calculations assume a source of 10^4 neutrons s^{-1} [1] at the center of the palladium rod. Results for any other neutron source level can be readily obtained since there is a directly proportional relationship. For example, an assumed source of 10^3 neutrons s^{-1} would lower all numerical values in Table 1 by a factor of 10. These energy dependent neutron flux values were computed using the Monte Carlo code "KENO" [4]. This code uses three-dimensional modeling and multiple discrete energy groups to represent the neutron cross sections as a function of energy. The Hansen–Roach [5] 16-group cross section set was utilized in this calculation. The neutron flux values computed as a function of energy also correspond to the same 16-group energy structure. The sum of these groups yields the total neutron flux level at the surface of interest. The kinetic energies of the neutrons decrease as the group number increases as shown in Table 1. The group 1 neutrons have more than seven orders of magnitude greater energies than the thermal neutrons of group 16.

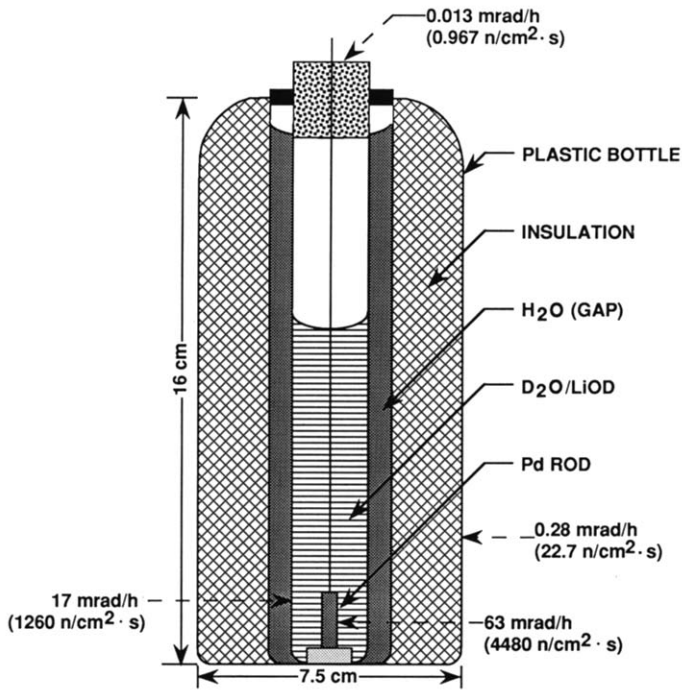

Fig. 1. Neutron flux and dose rates at the surface of the palladium rod, at the surface of the D_2O-filled electrochemical cell, at the side of the polyethylene bottle and at the top of the bottle. A source of 10^4 neutrons s^{-1} was assumed at the center of the palladium rod. The platinum coil electrode surrounding the palladium rod is not shown.

The neutron dose rates were computed by multiplying the neutron energy group flux values by corresponding Snyder–Auxier neutron tissue dose response functions [6]. These response functions have units of rad neutron^{-1} cm^{-2} (1 rad = 0.01 J/kg), hence the product of the flux times the response function when multiplied by 3600 s h^{-1} has units of rad h^{-1}. Table 2 presents the results of these calculations for each of the sixteen neutron energy groups at four different surfaces of the electrochemical calorimetric cell. The sum of these groups yields the total neutron dose rate at the four surfaces. The higher energy neutrons (lower group numbers) make the major contributions to the dose rates.

The neutron flux levels and dose rates computed for the surface of the palladium rod, the surface of the electrochemical cell, the outer surface of the polyethylene bottle, and the top of the stopper are shown in Fig. 1. The neutron dose rates at the outer surface of the bottle (0.28 mrad h^{-1}) and at the top of the bottle (0.013 mrad h^{-1}) suggest safe dose rates for people near the cold fusion experiment for a source of 10^4 neutrons s^{-1} within the palladium. Radiation exceeding weekly safe limits would not be reached even if the cold fusion bottle were held against the body for an entire 40-h work week. These calculations, however, indicate that neutron dose

TABLE 2

Neutron dose rates for the surface of the Pd rod, D_2O cell, side and top of the polyethylene bottle assuming a source of 10^4 neutrons per second

Group [a]	Dose rate/mrad h^{-1}			
	Pd surface	D_2O cell	Side of bottle	Top of bottle
1	2.179×10^{1}	4.664	9.265×10^{-2}	5.087×10^{-3}
2	2.014×10^{1}	7.505	8.794×10^{-2}	4.488×10^{-3}
3	8.951	1.982	3.682×10^{-2}	1.198×10^{-3}
4	8.571	2.017	3.890×10^{-2}	1.139×10^{-3}
5	2.902	7.752×10^{-1}	1.796×10^{-2}	5.632×10^{-4}
6	2.396×10^{-1}	8.213×10^{-2}	3.347×10^{-3}	1.276×10^{-4}
7	1.192×10^{-2}	1.198×10^{-2}	9.758×10^{-4}	3.400×10^{-5}
8	6.033×10^{-3}	7.141×10^{-3}	6.442×10^{-4}	3.285×10^{-5}
9	2.893×10^{-3}	4.320×10^{-3}	4.200×10^{-4}	2.224×10^{-5}
10	1.176×10^{-3}	2.004×10^{-3}	2.127×10^{-4}	2.174×10^{-5}
11	1.236×10^{-3}	1.265×10^{-3}	1.390×10^{-4}	7.704×10^{-6}
12	8.488×10^{-4}	9.175×10^{-4}	1.065×10^{-4}	9.281×10^{-6}
13	5.981×10^{-4}	5.815×10^{-4}	7.191×10^{-5}	5.848×10^{-6}
14	2.403×10^{-4}	2.496×10^{-4}	4.512×10^{-5}	7.823×10^{-6}
15	4.082×10^{-4}	5.887×10^{-4}	6.217×10^{-5}	3.763×10^{-6}
16	5.689×10^{-4}	7.573×10^{-4}	6.390×10^{-5}	8.622×10^{-6}
Totals	6.262×10^{1}	1.705×10^{1}	2.804×10^{-1}	1.276×10^{-2}

[a] Neutron energy range for each group is the same as in Table 1.

rates could be a health concern if there were a source of 10^6 neutrons s^{-1}. Neutron flux levels and dose rates would then be 100-fold greater than shown in Fig. 1 and Tables 1 and 2.

In addition to providing answers to safety concerns, these calculations show the best locations for the positioning of neutron detectors. Helium-3 and other neutron detectors respond mainly to thermal neutrons (Table 1, Group 16). The electrochemical cell portion of Fig. 1 is of a typical design, hence neutron flux levels and dose rates at the Pd surface and at the surface of the D_2O + LiOD electrolysis cell for other cold fusion experiments can likely be approximated by using Tables 1 and 2. Calculations for a particular cell and bottle design combined with experimental measurements of the thermal neutron flux make it possible to obtain the neutron source rate based on the assumed neutron energy spectrum (eqn. 2).

NEUTRON ACTIVATION OF METAL FOILS

The detection of neutrons in cold fusion experiments is difficult and controversial [1,3,7]. Various atmospheric or experimental conditions can yield spurious results when low neutron flux levels are measured. The activation of metal foils could be used to provide evidence of neutron generation by the cold fusion process that would be difficult to refute. Furthermore, metal foils can be readily positioned close

to the neutron source. Thermal neutrons (group 16, Table 1) would produce nearly all of this activation, hence Table 1 shows that the metal foil should be placed at the surface of the D_2O cell.

Metals selected for such activation experiments should have a naturally-abundant isotope with a large thermal neutron capture cross-section and should also yield radioactive products with half-lives measured in hours or days. Two excellent choices would be indium and gold foils (In-115, 95.7% natural abundance, 91.0 barns (1 barn = 10^{-24} cm^2/nucleus); Au-197, 100% natural abundance, 98.8 barns). Copper is another possible choice, but the cross-section is significantly smaller (Cu-63, 69.2% natural abundance, 4.5 barns; Cu-65, 30.8% natural abundance, 2.2 barns). All of these metals form isotopes upon neutron capture that are gamma-emitters with half-lives ranging from 5.1 min (Cu-65) to 2.693 days (Au-197). There are various metals that have much higher thermal neutron capture cross-sections than indium or gold, but they either yield stable products (Cd-113, 2.0×10^4 barns; Sm-149, 4.1×10^4 barns; Gd-157, 2.5×10^5 barns), have a low or nonexistent natural abundance, or involve the handling of radioactive and restricted materials (U-235, 580b). Dysprosium is an attractive choice (Dy-164, 28.2% natural abundance, 2.1×10^3b) except for its rather high chemical reactivity.

Calculations were performed to evaluate the possibility of activating copper, indium, and gold foils with the thermal neutron flux levels (group 16, Table 1) likely to be encountered at various surfaces of the cold fusion bottle. Table 1 suggests that the metal foil should be mounted at the surface of the D_2O-filled electrochemical cell where the thermal neutron flux is 0.4068 n cm^{-2} s^{-1}. This value is even higher than the thermal neutron flux near the surface of the palladium rod (Table 1).

In a typical experiment with a 30-day duration, copper, indium, and gold foils would all reach their maximum or saturation activity given by

$$A = \phi\sigma N \tag{3}$$

where ϕ is the thermal neutron flux, σ is the thermal neutron absorption cross-section, and N is the atom density. Table 3 shows the cross-section and atom density values for Cu-63, In-115, and Au-197 along with the saturation activity for each foil exposed to the thermal neutron flux level of 0.4068 n cm^{-2} s^{-1} as computed with

TABLE 3

Saturation activity values for copper, indium, and gold foils placed at the outer glass surface of the D_2O-filled electrochemical cell

Metal foil	Thermal neutron flux/n cm^{-2} s^{-1}	Cross section /barn [b]	Atom density [a] /atom b^{-1} cm^{-1}	Saturation activity /dis s^{-1} cm^{-3}
Cu-63	0.4068	4.5	0.05877	0.108
In-115	0.4068	91.0	0.03670	1.359
Au-197	0.4068	98.8	0.05902	2.372

[a] Includes correction for natural abundance.
[b] 1 barn = 10^{-24} cm^2/nucleus.

KENO for the surface of the D_2O-filled electrochemical cell (Table 1). These data suggest that indium or gold foils mounted at the surface of the electrochemical cell could activate sufficiently to provide additional evidence of neutron generation by the cold fusion process. The neutron emission rate, however, needs to be at least 10^5 neutrons s^{-1} in order to activate gold or indium foils placed on the outer surface of the cold fusion bottle. The saturation activity for copper will always be significantly smaller than for gold or indium and more difficult to detect.

The palladium cathode was also considered for possible activation since the neutrons are produced within its metal lattice. The various naturally-occurring isotopes of palladium have rather small thermal neutron capture cross-sections; therefore, their calculated saturation activities from eqn. 3 are too small for experimental detection. The Pd-108 isotope (26.7% natural abundance, 0.20b) gave the highest saturation activity, but this was only 0.0011 dis s^{-1} cm^{-3} when the thermal neutron flux at the palladium surface (0.3056 n cm^{-2} s^{-1}) is used. The theoretical calculations in this study suggest that any transmutation of palladium during cold fusion experiments will be very difficult to detect. Even if all of the 10^4 n s^{-1} were absorbed by the palladium cathode, it would require more than 200 years to produce one part-per-billion isotopic change or transmutation in 1 cm^3 volume of palladium.

ACKNOWLEDGEMENT

The authors thank Larry Liedtke for helpful discussions relating to metal activation.

REFERENCES

1 M. Fleischmann, S. Pons and M. Hawkins, J. Electroanal. Chem., 261 (1989) 301; err. 263 (1989) 187.
2 M.H. Miles, K.H. Park and D.E. Stilwell, Proceedings of the First Annual Conference on Cold Fusion, Salt Lake City, UT, March 1990, pp. 328—334; J. Electroanal. Chem., 296 (1990) 255.
3 S.E. Jones, E.P. Palmer, J.B. Czirr, D.L. Decker, G.L. Jensen, J.M. Thorne, S.F. Taylor and J. Rafelski, Nature, 338 (1989) 737.
4 L.M. Petrie and N.F. Cross, KENO–IV—An Improved Monte Carlo Criticality Program, ORNL-4938, Oak Ridge National Laboratory, November 1975.
5 G.E. Hansen and W.H. Roach, Six and Sixteen Group Cross Sections for Fast and Intermediate Critical Assemblies, LAM-2543, Los Alamos National Laboratory, 1961.
6 D.E. Bartine, J.R. Knight, J.V. Pace III and R.W. Roussin, Production and Testing of the DNA Few-Group Coupled Neutron-Gamma Cross-Section Library, ORNL/TM-4840, Oak Ridge National Laboratory, March 1977.
7 R.D. Petrasso, X. Chen, K.W. Wenzel, R.R. Parker, C.K. Li and C. Fiore, Nature, 339 (1989) 183.